

Phenolic foams toughened with crosslinked poly (n-butyl acrylate)/silica core-shell nanocomposite particles

Junjie Yuan,^{1,2} Yunbo Zhang,¹ Zhengzhou Wang^{1,2}

¹Department of Polymer, School of Materials Science and Engineering, Tongji University, Shanghai 201804, People's Republic of China

²Key Laboratory of Advanced Civil Engineering Materials, Ministry of Education, Tongji University, Shanghai 201804, People's Republic of China

Correspondence to: J. Yuan (E-mail: yuanjunjie@tongji.edu.cn)

ABSTRACT: A new type of crosslinked poly (n-butyl acrylate) (PBA)/silica core-shell nanocomposite particles was adopted as toughening agent to improve the mechanical properties of phenolic foams. The effects of the nanocomposite particles on the structures and properties of lightweight phenolic foams were investigated. SEM result showed that the addition of a small quantity of the nanocomposite particles can significantly enhance the structural homogeneity of phenolic foams. Thermalgravimetric analysis result suggested that the incorporation of the nanocomposite particles did not affect the thermal stability of the toughened phenolic foams. The flexural strength, compressive strength, and elastic modulus of the phenolic foams increased distinctively after the addition of the nanocomposite particles, the maximum values of which increased by 36.0%, 42.9%, and 32.3%, respectively. In this study, the optimum dosage of the nanocomposite particles is 0.03 phr in the modified phenolic foams. Moreover, the influence on the flammability of phenolic foams by toughening can almost be neglected. © 2015 Wiley Periodicals, Inc. *J. Appl. Polym. Sci.* **2015**, *132*, 42590.

KEYWORDS: composites; foams; mechanical properties; nanoparticles; nanowires and nanocrystals

Received 28 October 2014; accepted 3 June 2015

DOI: 10.1002/app.42590

INTRODUCTION

Polyurethane foam and polystyrene foam are widely used in thermal insulation materials for buildings. However, due to their high flammability, replacing them with phenolic foams is a common trend.¹ Due to its low thermal conductivity, excellent flame-retardant performance, affordable cost, high dimensional stability, low generation of toxic gas and no dripping during combustion, phenolic foam has been extensively studied in recent years.^{2–4} It is very suitable for the application in insulating and structural materials where fire resistance is critical.⁵ Nevertheless, it is highly brittle and fragile friability that seriously restricts its wide applications. Therefore, the toughening of phenolic foams is essential for the application of them.

Many methods were explored for the toughening of phenolic foams. For example, many researchers adopted modified phenols which possess flexible chains such as cardanol phenolic resin^{6,7} and linseed phenolic resin^{8,9} instead of phenol to synthesize phenolic resin, and obtained toughened phenolic foams. Some researchers made use of polyurethane,^{10,11} epoxy,^{12,13} and polyethylene glycol¹⁴ to react with resol resin for toughening phenolic foams. Some investigators directly mixed rubbers^{15,16}

and fibers^{17–20} into foaming system to toughen phenolic foams. Although organic toughening agents can effectively improve the toughness of the phenolic foams, they tend to destroy the flame-retardant properties of phenolic foams. Flame-retardant properties of most modified phenolic foams with organic materials substantially decreased. Inorganic particles are candidates of the toughening agents for phenolic foams. For instance, attapulgite,²¹ hollow carbon microsphere,²² and activated carbon²³ were investigated to toughen phenolic foams. However, the addition of inorganic toughening agents often increases the viscosity of phenolic resin which has negative effect on the foaming process.

In order to retain superior flame-retardant properties of phenolic foams while enhancing the toughening properties, prepolymer containing P and N elements were adopted to modify phenolic foam. For example, Sui and Wang¹⁴ synthesized several different kinds of polyethylene glycol phosphates (PEGPs) toughening agents which were mixed with phenolic resin to prepare phenolic foams. The results indicated that the incorporation of PEGPs not only increased the toughness of phenolic foams but also improved their flame retardancy. Hu *et al.*^{1,24} synthesized phosphorus-containing polyurethane prepolymer

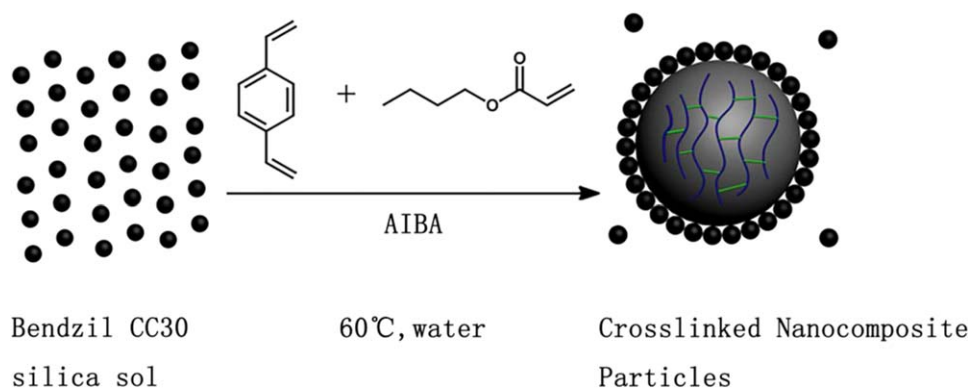


Figure 1. Schematic synthesis route of nanocomposite particles by emulsion polymerization of n-butyl acrylate using a cationic azo initiator in the presence of a commercial aqueous glycerol-functionalized silica sol as the sole stabilizing agent. [Color figure can be viewed in the online issue, which is available at wileyonlinelibrary.com.]

and phosphorus-containing polyethers to toughen phenolic foams. They have found that the addition of phosphorus- and silicon-containing polyurethane prepolymer (PSPUP) and phosphorus-containing polyether can increase the compressive strength of the modified phenolic foams and the optimum dosage of these two toughening agents is 5 wt %. The limiting oxygen index values of modified phenolic foams decreased with the increases of modifiers content, but still above 40% even if the amount of modifiers loadings was 5 wt %. As discussed above, it is well known that inorganic materials possess excellent flame-retardant and mechanical properties. So incorporation of inorganic materials with organic materials is a promising way to modify phenolic foams. For instance, Yuan *et al.*²⁵ found that the modified phenolic foams with 3 wt % phosphorus-containing polyurethane prepolymer (DOPU) and 0.5 wt % glass fiber exhibited good thermal stability and high char yields. The limiting oxygen index value of modified phenolic foams decreased with increasing DOPU content. Therefore, the additives which can improve the toughness and does not deteriorate the flame-retardant performance at the same time are expected.

Nanocomposite particles composed of silica and polymer have been extensively studied recently due to their superior thermal, mechanical, optical, magnetic, and electrical properties, which are derived from the synergy between the two components.^{26,27} Polymer/silica nanocomposite particles with core-shell structure are most important. This kind of nanocomposite particles can be fabricated as soft polymer core-hard silica shell structure which is very similar to that of traditional core-shell toughening agent. However, based on our knowledge, little research has been devoted to the toughening of phenolic foams with this kind of nanocomposite particles.

In this work, a kind of weakly crosslinked poly(n-butyl acrylate)/silica core-shell nanocomposite particles were prepared via aqueous emulsion polymerization. The shell is composed of nanosilica particles with hydroxyl groups, which can react with hydroxyl groups of phenolic resin and provide good compatibility with phenolic resin. The core consists of poly(n-butyl acrylate), like rubber, can absorb part of the impact energy. So toughening phenolic foams with these core-shell structure nanocomposite particles can be expected. The structure and prop-

erties of phenolic foams with different loadings of the nanocomposite particles were examined in detail.

EXPERIMENTAL

Materials

The commercial glycerol-functionalized silica sols (Bindzil CC30, nominal 7 nm diameter, 30 wt %) was obtained from AkzoNobel Industrial Chemicals. Butyl acrylate (Analytical Reagent), divinylbenzene (DVB, 80 wt %) and 2,2'-azobis(2-methylpropionamide) dihydrochloride (AIBA) were supplied by Aladdin Industrial Corporation (Shanghai, China). Phosphoric acid (Analytical Reagent), p-toluenesulfonic acid (Analytical Reagent), n-pentane (99.6%), n-butyl acrylate (Chemically Pure) and Tween 80 were all purchased from Sinopharm Chemical Reagent Corporation (Shanghai, China). The resol resin was supplied by Shandong Shengquan Chemical (Shandong, China).

Synthesis of PBA/Silica Core-Shell Nanocomposite Particles

Aqueous silica sol (10.0 g) was diluted with 36.0 g of deionized water and placed in a three-necked flask containing a magnetic stirrer. Then, 3.3 g of n-butyl acrylate and 0.0042 g of divinylbenzene were added. The mixture was strongly stirred and degassed by two evacuation/nitrogen purge cycles at room temperature and subsequently heated to 60°C in an oil bath. The AIBA (33.0 mg) was dissolved in water (4.0 g) before added to the flask.²⁸ The polymerization reaction was maintained for 24 h. The milky-white colloidal dispersions were obtained. The schematic synthesis process is shown in Figure 1.

Preparation of Phenolic Foams Modified with PBA/Silica Core-Shell Nanocomposite Particles

The mixture of resol resin and PBA/silica core-shell nanocomposite particles was heated up to 80°C for 1 h and cooled to room temperature before using. The processed resol resin, Tween-80, curing agent (mixture of phosphoric acid, p-toluenesulfonic acid and water, pH = 0.68), and n-pentane were mixed together rapidly and strongly with a mixer at a certain proportion for about 5 min. Then, the viscous mixture was quickly poured into a cuboid mold which can be sealed and cured at 80°C for 40 min. For each molding, the same amount of the mixture was put into the mold

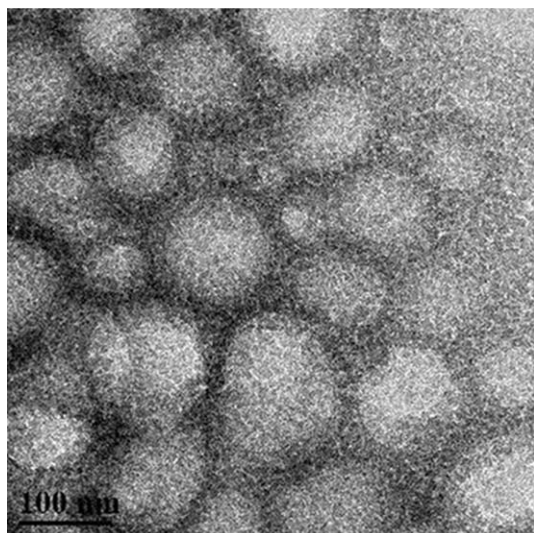


Figure 2. TEM images of nanocomposite particles prepared by emulsion polymerization in the presence of a glycerol-modified silica sol (Bendzil CC30). Polymerization was conducted using 3.3 g n-butyl acrylate, 10.0 g silica sol (3.0 g dry silica), 4.2 mg DVB and 33 mg AIBA initiator at 60°C for 24 h. The images reveal that nanocomposite particles possess a distinct core-shell morphology, the polymer component forms the core and the silica particles form the shell. Particle coalescence can also be observed.

to obtain the relatively uniform density of foams. The samples were cut discreetly for mechanical, fire and other tests.

Characterization

Particle Size Analysis. Dynamic Light Scattering (DLS, Malvern Instruments ZS 90) was used to characterize the particle size and distribution of PBA/silica nanocomposite particles.

Transmission Electron Microscopy (TEM). The diluted silica/PBA nanocomposite latex was ultrasonicated for 5 min and then dried onto carbon-coated copper grids before examination. Analysis was conducted using a JEOL-2100F TEM instrument operating at 200 kV.

Scanning Electron Microscopy (SEM). SEM (Hitachi Co., Japan) was used to observe the cellular structure of phenolic foams, which was obtained by thin sectioning.

Cell Size and Cell Density Tests. Average cell diameter was calculated by Image Pro software from SEM photographs of phenolic foams. The cell density was given by

$$N_f = \left(\frac{nM^2}{A} \right)^{\frac{3}{2}} \times \frac{\rho}{\rho_f}$$

where, A , area of SEM photograph; M , magnification of SEM; n , cell numbers in A ; ρ , density of curried phenolic resin; ρ_f , density of phenolic foam.

Thermogravimetric and Differential Scanning Calorimetric Analysis (TGA and DSC). The samples were analyzed by TGA instrument (Perkin-Elmer TGA-7) in air from room temperature to 800°C at a rate of 20°C/min. Differential scanning calorimetric (DSC) experiments were carried out using a Q2000 DSC (TA Co., America) with temperature ranging from 30°C

to 400°C at a heating rate of 10°C/min under nitrogen atmosphere.

Mechanical Properties and Apparent Density Tests. Mechanical properties of phenolic foams were evaluated by bending test with a DXLL-5000 universal testing machine (Shanghai D&G Machinery Equipment, China) according to GB/T 8812.1-2007 and compression test with a CMT 5105 universal testing machine (Shenzhen sans testing machine, China) according to GB/T 8813-2008. The specimen dimensions of bending test and compression test were $120 \times 25 \times 20 \text{ mm}^3$, $30 \times 30 \times 30 \text{ mm}^3$ respectively. The deformation velocities of bending test is 10 mm/min and compression test is 3 mm/min. At least five replicates were tested for each specimen. The apparent density was determined using the dimensions and the weight of dried foams.

Limiting Oxygen Index (LOI) Test. The samples were conducted with an HC-2 oxygen index meter (Jiangning Analysis Instrument, China) according to the ASTM D2863. The specimen dimensions of LOI test was $100 \times 10 \times 10 \text{ mm}^3$.

RESULTS AND DISCUSSION

Morphologies and Structure of Silica/PBA Core-Shell Nanocomposite Particles

The TEM image of PBA/Silica core-shell nanocomposite particles is demonstrated in Figure 2. It can be clearly seen that core-shell structure nanocomposite particles are formed. Lots of small silica particles are coated on the surface of PBA core particles. The nanocomposite particles almost all adhere together probably due to crosslinking effect of soft monomer butylacrylate in the core of the nanocomposite particles. DLS result indicates that the average hydrodynamic diameter of the nanocomposite particles is about 178.9 nm with the particle dispersion index (PDI) of 0.171, as displayed in Figure 3.

Microstructures of Modified Phenolic Foams

The properties of phenolic foams strongly depend on their individual density.²⁹ A series of modified phenolic foams with the approximately same apparent density were prepared to study the effects of the dosage of nanocomposite particles on the properties of phenolic foams. It is worth emphasized that the

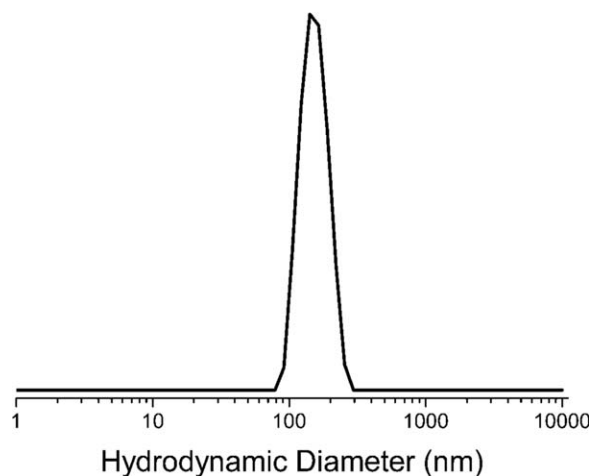


Figure 3. The hydrodynamic diameter of nanocomposite particles.

Table I. Formulation of Phenolic Foams and Effect of Varying the Nanocomposite Particles Content on Apparent Density, T_g , Cell Average Diameter, Cell Density of Phenolic Foams

Sample	Content of nanoparticles (phr)	Content of resin (phr)	Apparent density (kg/m ³)	Average cell diameter (μm)	Cell density (10 ⁷ cells/cm ³)	T_g (°C)
PF0	0	100	24.6	96.5	8.6	169.4
PF1	0.015	100	24.9	80.6	13.8	171.2
PF2	0.03	100	24.9	72.4	18.4	170.4
PF3	0.06	100	25.0	90.3	13.3	172.7
PF4	0.09	100	25.2	98.7	8.5	171.6
PF5	0.12	100	25.4	104.0	7.5	174.3
PF6	0.15	100	25.1	115.4	6.7	186.5

Blowing agent, 7 phr; curing agent, 8 phr; surfactant, 4 phr.

apparent density of all the foams is around $25 \pm 0.5 \text{ kg/m}^3$, which is lower than that of phenolic foams reported earlier (270, 314, 200, 60, 100 kg/m³),^{3,30–33} as shown in Table I. The microstructure of the pure phenolic foam and the modified phenolic foams with nanocomposite particles are characterized by SEM, as shown in Figure 4. The cells distribution and shape of the modified foams become more regular and uniform than that of pure phenolic foam when the amount of nanocomposite particles increases from 0.015 phr to 0.09 phr. However, the cells structure of foams becomes more distorted and irregular than that of the pure phenolic foam when the amount of nanocomposite particles increases to 0.12 phr and 0.15 phr. The results illustrate that the appropriate addition of nanocomposite particles can improve the structural homogeneity of phenolic foams. The cell size and cell density of phenolic foams are shown in Table I. The cell size of phenolic foam increases when the dosage of nanosilica increases from 0 phr to 0.06 phr and decreases when the dosage of nanosilica increases from 0.09 phr to 0.15 phr. The tendency of cell density is contrary to cell size. It can be seen that there are many particles are dispersed in the cell walls of phenolic foam in the Figure 4(h). The diameters of these particles are about 450–700 nm which are larger than that of the single nanosilica particles. It is supposed that there occurs to aggregate when the nanosilica particles are added in the system.

With increasing the dosage of the nanoparticles, the viscosity of the processed resin rises. In the foaming process, the blowing

agent is vaporized by heating to produce small bubbles. As the temperature rises, the pressure of small bubbles becomes larger. The bubbles become bigger until the cell wall ruptures. Then the perforated structure is formed. This moment, a foam homogenizing process occurs to form a uniform cell structure due to the certain fluidity of the resin. Meanwhile, the suitable viscosity of the resin could maintain the cell structure without rupture. After the curing process, the foam with uniform cell structure could be obtained. If the viscosity is not enough, the uniform cell structure could not be maintained well. Otherwise, if the viscosity is too high, it will be difficult to accomplish the homogenizing process. So the homogeneity of the cell structure can be improved by increasing the viscosity of the resin appropriately. However, the excessively high viscosity will go against the homogeneity of the cell structure.

Thermal Decomposition Performance of Modified Phenolic Foams

Figures 5 and 6 show the TGA and DTG curves of phenolic foams with various contents of nanocomposite particles at the linear heating rate of 20°C/min under nitrogen atmosphere. And some TGA and DTG data of phenolic foams were shown in Table 2. All phenolic foams present the similar degradation behavior. In Figure 6, it can be seen that there are four maximum degradation temperatures which are mainly caused by the evaporation of water (a), evaporation of Tween 80 and free phenol (b), dehydration of dibenzyl ether bond (c), and degradation of phenolic resin (d), respectively. The temperature at 5% mass loss ($T_{-5\%}$), fastest dehydration of dibenzyl ether bonds (T_c), fastest degradation of phenolic resin (T_d) and initial degradation of phenolic resin (T_e) was displayed in Table I. $T_{-5\%}$ of PF2 and $T_{-5\%}$ of PF3 are much higher than others due to the lower initial water and free methanol content. Thus the proportion of other components is higher than other samples. However, it doesn't influence the analysis of degradation properties of phenolic foams. Compared with PF0, $T_{c,s}$ of PF1, PF2, PF3, and PF4 are just slightly higher. Nevertheless, $T_{c,s}$ of PF5 and PF6 are much higher than other samples. In Table I, we can see that the cell densities of PF5 and PF6 are very low. The cell walls must be very thick due to the closed foaming system. The water deriving from dehydration of dibenzyl ether bonds is difficult to evaporate. Thus the endothermic process will be postponed. Whatever, it almost doesn't change in the T_d and

Table II. Some TGA and DTG Data of Phenolic Foams

Sample	$T_{-5\%}$ (°C)	T_c (°C)	T_d (°C)	T_e (°C)
PF0	158.3	301.5	482.4	410.2
PF1	201.9	303.5	482.7	412.6
PF2	257.5	304.4	484.1	413.7
PF3	266.2	304.6	478.7	412.2
PF4	176.5	305.1	479.8	413.1
PF5	182.7	392.5	484.8	414.8
PF6	183.3	393.3	488.4	414.5

$T_{-5\%}$, the temperature at 5% mass loss; T_c , temperature at fastest dehydration of dibenzyl ether bonds; T_d , temperature at fastest degradation of phenolic resin; T_e , temperature at initial degradation of phenolic resin.

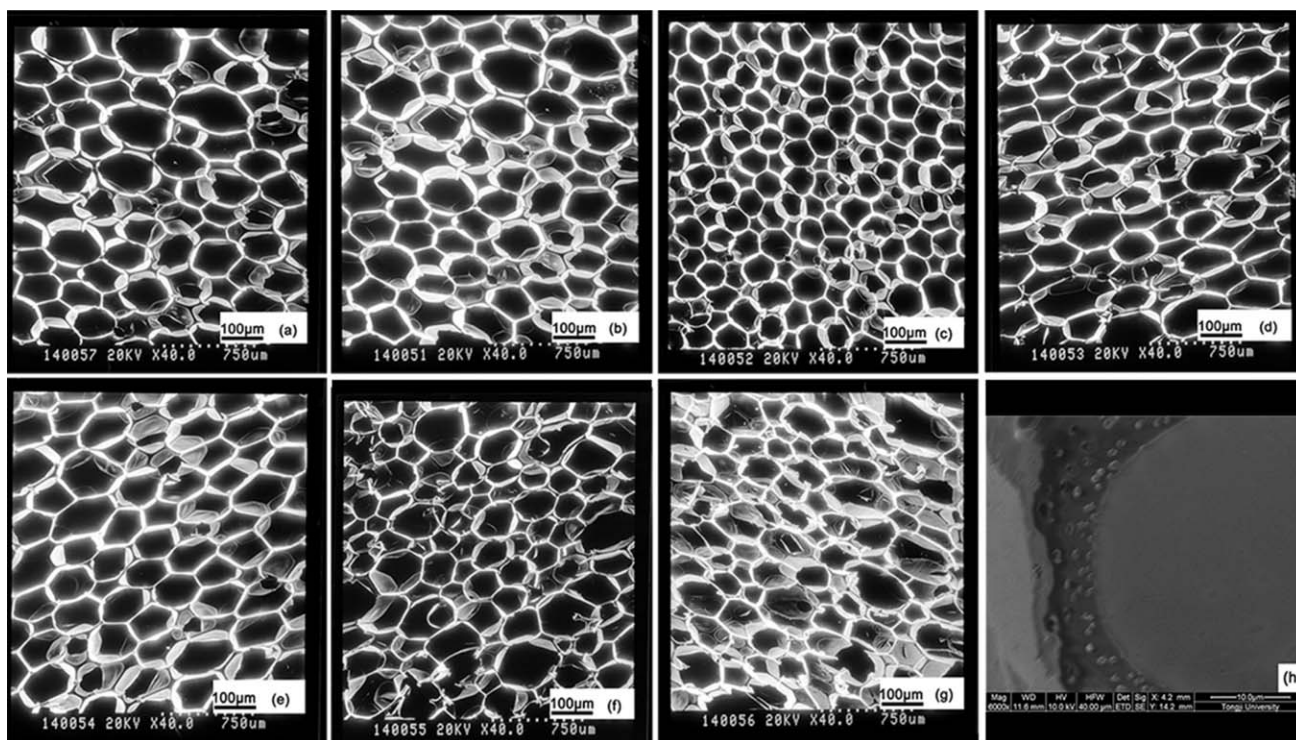


Figure 4. SEM micrographs of the phenolic foams with different content of nanocomposite particles: (a) 0 phr; (b) 0.015 phr; (c) 0.03 phr; (d) 0.06 phr; (e) 0.09 phr; (f) 0.12 phr; (g) 0.15 phr. The images were magnified 40 times. The image (h) was magnified 6000 times of the phenolic foam with nanocomposite particles of 0.06 phr.

T_g of phenolic foams which suggests the addition of nanocomposite particles does not damage the heat resistance property of phenolic foams.

Glass Transition Temperature of the Modified Phenolic Foams

Glass transition temperature (T_g) of the phenolic foams is obtained from the DSC curves, as displayed in Figure 7. T_g data of these samples are listed in the Table I. T_g of the modified

phenolic foams increases slightly with increasing nanoparticles content from 0.015 phr to 0.12 phr. However, the T_g of phenolic foams distinctively increases when the dosage of nanosilica particles is 0.15 phr. Maybe it is caused by the viscosity saltation of phenolic resin when 0.15 phr nanosilica particles are added into the system. The results indicate the addition of nanocomposite particles has little effect on T_g of the pure phenolic foam. Usually, T_g of the polymer matrix increases when nanoparticles

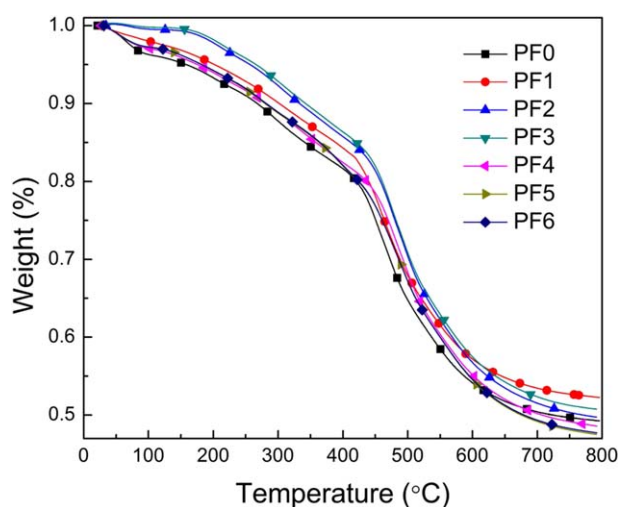


Figure 5. TGA curves of phenolic foams used different nanocomposite particles content. [Color figure can be viewed in the online issue, which is available at wileyonlinelibrary.com.]

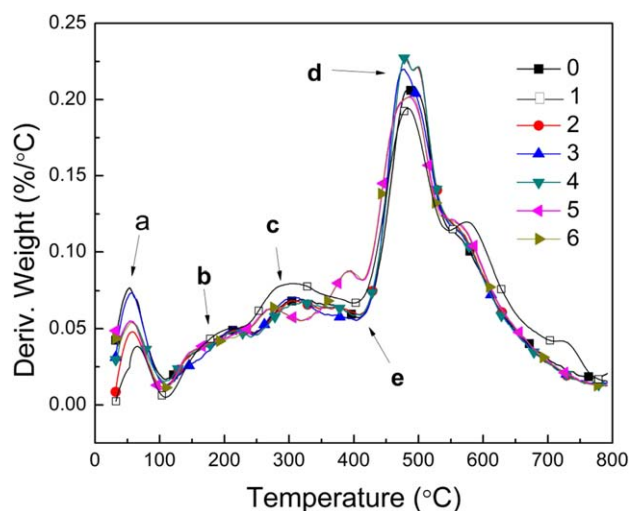


Figure 6. DTG curves of phenolic foams used different nanocomposite particles content. [Color figure can be viewed in the online issue, which is available at wileyonlinelibrary.com.]

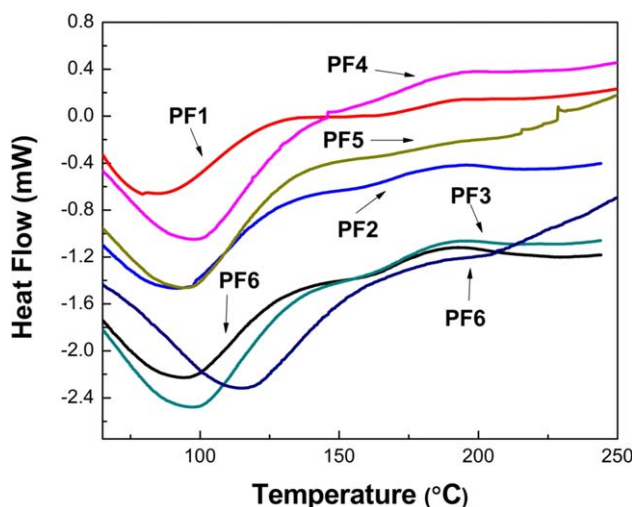


Figure 7. DSC curves of phenolic foams used different nanocomposite particles content. [Color figure can be viewed in the online issue, which is available at wileyonlinelibrary.com.]

is incorporated into a polymer matrix, because the addition of nanoparticles hinders the motion of the polymer chains. For instance, Rangari *et al.*³⁰ found that the incorporation of cloisite clay nanoparticles increased the T_g of modified phenolic foams. This attributes to the higher crosslinking density of modified phenolic foams. However, in our system, it does not change much. This is probably because the crosslinking degree of the pure phenolic foam is very high and the content of nanoparticles is too low. After the nanocomposite particles are added into the system, the total crosslinking degree of the modified phenolic foams doesn't change distinctively. Therefore, the addition of nanocomposite particles has a limited influence on T_g of the modified phenolic foams.

Mechanical Properties

The elastic modulus and flexural and compressive strength of the pure phenolic foam and the toughened phenolic foams with nanocomposite particles are illustrated in Figures 8 and 9, respectively. It is found that the elastic modulus and flexural and compressive strength of the toughened foams increase rapidly at first and reach the maximum when the dosage of nanocomposite particles is 0.03 phr. The phenolic foam containing 0.03 phr nanocomposite particles has the highest elastic modulus (2.491 MPa), flexural strength (0.209 MPa) and compressive strength (0.08 MPa), which increases significantly by 32.3%, 36.0%, and 42.9%, respectively compared with that of pure phenolic foam. When the dosage is higher than 0.03 phr, the elastic modulus and flexural and compressive strength of the modified phenolic foams begin to decrease. Nevertheless, the foams containing 0.015 phr, 0.06 phr, and 0.09 phr nanocomposite particles still have the higher elastic modulus and flexural and compressive strength compared with that of the pure phenolic foam. The elastic modulus and flexural and compressive strength of foams containing 0.12 phr and 0.15 phr particles are lower than that of the pure phenolic foam. The results are highly consistent with the result of the SEM.

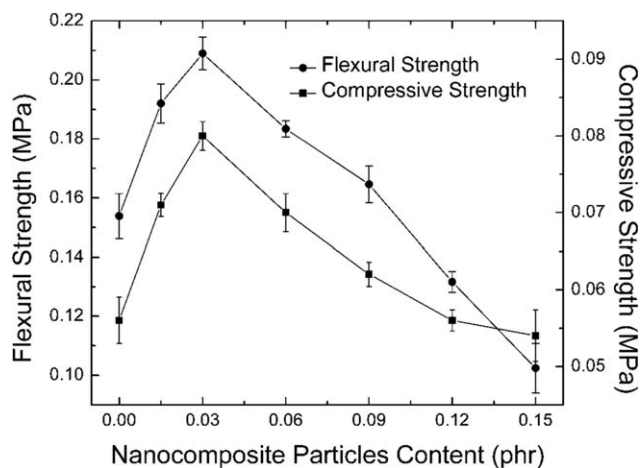


Figure 8. Effect of nanocomposite particles content on the elastic modulus of phenolic foams.

Generally, the toughness can be characterized by the area under the stress-strain curve. The bigger area indicates better toughness of the sample possesses. In Figure 10, the areas of PF1, PF2, PF3, and PF4 under the curves are bigger than that of PF0, whereas the areas of PF5 and PF6 are smaller than that of PF0.

A probable explanation is based on the overacted condensation between the hydroxyl groups on the surface of particles and hydroxymethyl groups of the phenolic resol. The excessive consumption of crosslinking points in the system leads to the generation of methylene bridges, which are reduced in curing process. So incorporation with too much nanocomposite particles can deteriorate the curing process and formation of the network structure, even form some defects and fissures. Typically, these defects and fissures are prone to cause stress concentration and become the weakness of materials, thereby turn to severely reduce the flexural and compressive strength of phenolic foam. On the other hand, the viscosity of the processed resol resin

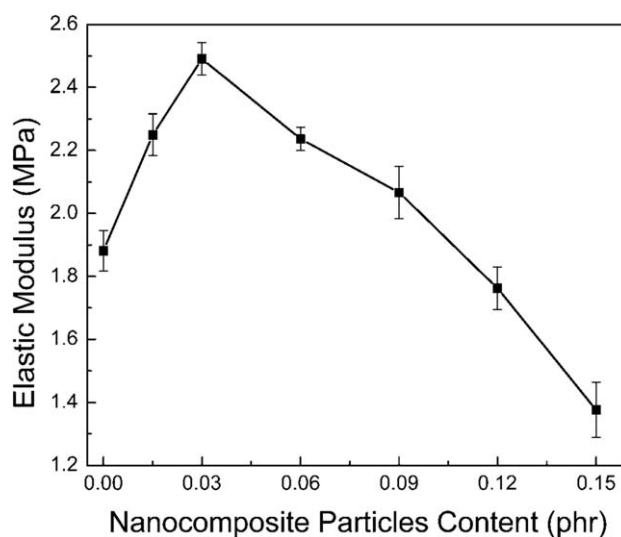


Figure 9. Effect of nanocomposite particles content on the flexural and compressive strength of phenolic foams.

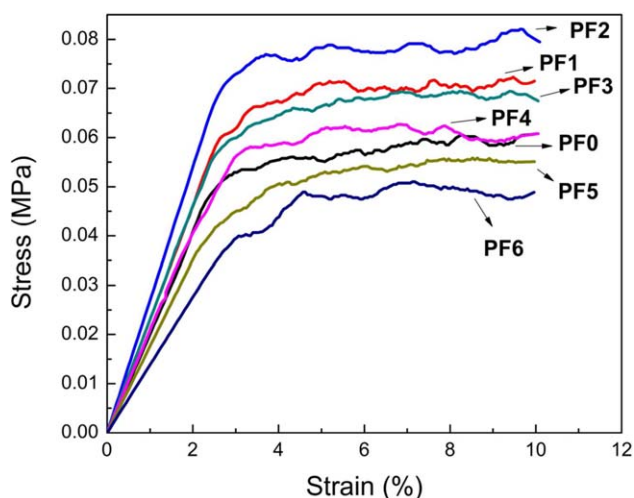


Figure 10. Compressive stress-strain relationships of the phenolic foams. [Color figure can be viewed in the online issue, which is available at wileyonlinelibrary.com.]

rises with increment of the dosage of the nanoparticles and results in aggregates of the additives in the system. When the dosage of the nanocomposite particles is higher than 0.15 phr, the viscosity of the system is too high to disperse the additives uniformly and the foam collapses.

Attributing to the existence of an abundant of hydroxyl groups on the surface, nanocomposite particles may react with the polymer to form a strong interfacial interaction. When the condensation reaction between the hydroxyl groups on the surface of particles and hydroxymethyl groups of the phenolic resin takes place, the covalent bond will form and in turn improve the interface compatibility of phenolic matrix and nanocomposite particles greatly. As the core of nanocomposite particles, poly (n-butyl acrylate) can absorb energy when the phenolic foam is impacted. All these can bring in significant improvement in the toughness of phenolic foam.

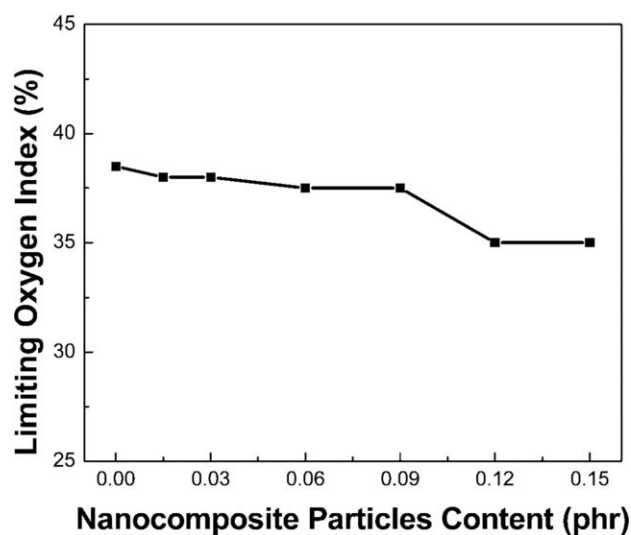


Figure 11. Effect of nanocomposite particles content on the limit oxygen index of phenolic.

Flame-Retardant Performance of Modified Phenolic Foams

The flammability of the pure phenolic foam and modified phenolic foams with nanocomposite particles is evaluated by limiting oxygen index (LOI) test. The results are shown in Figure 11. No obvious effect on LOI is observed when the dosage of nanocomposite particles increases from 0.015 phr to 0.09 phr. However, when the amount of nanocomposite particles is above 0.12 phr, LOI decreases slightly. In our designed system, the addition of nanocomposite particles has a tiny effect on LOI of phenolic foams. Excellent flame-retardant performance of modified phenolic foams is still retained, while the toughness of the phenolic foam is improved. The result is understandable because the dosage of nanocomposite particles is very small.

CONCLUSIONS

A series of nanocomposite particles toughening agents were successfully synthesized to modify phenolic foams. SEM result showed that the nanocomposite particles greatly improved the structural homogeneity of phenolic foams when the dosage was less than 0.09 phr. The flexural and compression strength results prove that with the increase of dosage of nanocomposite particles, they first increase and then decrease. The optimum dosage is 0.03 phr in our present study. Compared with that of pure phenolic foam, flexural strength, compressive strength and elastic modulus were increased by 36.0%, 42.9%, and 32.3%. TGA result indicates that nanocomposite particles lead to a slight increase in the heat resistance of phenolic foams. The LOI result demonstrates that the incorporation of nanocomposite particles will not damage the excellent flame-retardant performance of phenolic foam.

ACKNOWLEDGMENTS

This work was financially supported by the National Natural Science Foundation of China (50803046, 21174106 and U1205114/L11). The project was also sponsored by the foundation of Key Laboratory of Advanced Civil Engineering Materials, Tongji University.

REFERENCES

1. Yang, H.; Wang, X.; Yu, B.; Yuan, H.; Song, L.; Hu, Y.; Yuen, R. K.; Yeoh, G. H. *J. Appl. Polym. Sci.* **2013**, *128*, 2720.
2. Shen, H.; Nutt, S. *Compos. Part A* **2003**, *34*, 899.
3. Lei, S.; Guo, Q.; Zhang, D.; Shi, J.; Liu, L.; Wei, X. *J. Appl. Polym. Sci.* **2010**, *117*, 3545.
4. Lei, S.; Guo, Q.; Shi, J.; Liu, L. *Carbon* **2010**, *48*, 2644.
5. Del Saz-Orozco, B.; Alonso, M. V.; Oliet, M.; Dominguez, J. C.; Rodriguez, F. *Compos. B* **2014**, *56*, 546.
6. Parameswaran, P. S.; Abraham, B. T.; Thachil, E. T. *Prog. Rubber Plast. Recycl. Technol.* **2010**, *26*, 31.
7. Niu, M.; Wang, G. J. *Adv. Mater. Res.* **2013**, *712*, 147.
8. Cayli, G.; Kusefoglu, S. *J. Appl. Polym. Sci.* **2010**, *118*, 849.
9. Michotte, D.; Rogez, H.; Chirinos, R.; Mignolet, E.; Campos, D.; Larondelle, Y. *Food Chem.* **2011**, *129*, 1228.

10. Wu, H. D.; Lee, M. S.; Wu, Y. D.; Su, Y. F.; Ma, C. C. M. *J. Appl. Polym. Sci.* **1996**, *62*, 227.
11. Li, T.; Zhang, L.; Jiang, H. M.; Chen, J. Z.; Li, X. F. TNCPE 13, Aug 21–26, **2010**, Wuhan, People Republic China.
12. Auad, M. L.; Zhao, L. H.; Shen, H. B.; Nutt, S. R.; Sorathia, U. *J. Appl. Polym. Sci.* **2007**, *104*, 1399.
13. Lu, S. H.; Zhou, Z. W.; Fang, L.; Liang, G. Z.; Wang, J. L. *J. Appl. Polym. Sci.* **2007**, *103*, 3150.
14. Sui, X.; Wang, Z. *Polym. Adv. Technol.* **2013**, *24*, 593.
15. Kaynak, C.; Cagatay, O. *Polym. Test.* **2006**, *25*, 296.
16. Yu, Z.; Li, J. F.; Yang, L. M.; Yao, Y. L.; Su, Z. Q.; Chen, X. N. *J. Appl. Polym. Sci.* **2012**, *123*, 1079.
17. Paiva, J. M. F.; Frollini, E. *Macromol. Mater. Eng.* **2006**, *291*, 405.
18. Megiatto, J. D.; Silva, C. G.; Rosa, D. S.; Frollini, E. *Polym. Degrad. Stab.* **2008**, *93*, 1109.
19. Wouterson, E. M.; Boey, F. Y.; Hu, X.; Wong, S. C. *Polymer* **2007**, *48*, 3183.
20. Shen, H. B.; Nutt, S. *Compos. A* **2003**, *34*, 899.
21. Zhuang, Z. H.; He, B.; Yang, Z. G. *Plast. Rubber Compos. Process. Appl.* **2010**, *39*, 460.
22. Zhang, L. Y.; Ma, J. *Compos. Sci. Technol.* **2010**, *70*, 1265.
23. Song, S. A.; Oh, H. J.; Kim, B. G.; Kim, S. S. *Compos. Sci. Technol.* **2013**, *76*, 45.
24. Yang, H. Y.; Wang, X.; Yuan, H. X.; Song, L.; Hu, Y.; Yuen, R. K. K. *J. Polym. Res.* **2012**, *19*.
25. Yuan, H. X.; Xing, W. Y.; Yang, H. Y.; Song, L.; Hu, Y.; Yeoh, G. H. *Polym. Int.* **2013**, *62*, 273.
26. Pourhossaini, M. R.; Razzaghi-Kashani, M. *Polymer* **2014**, *55*, 2279.
27. Zeyghami, M.; Kharrat, R.; Ghazanfari, M. H. *Energy Sources Part A* **2014**, *36*, 1315.
28. Schmid, A.; Scherl, P.; Armes, S. P.; Leite, C. A.; Galembeck, F. *Macromolecules* **2009**, *42*, 3721.
29. Sui, X. Y.; Wang, Z. Z. *Polym. Adv. Technol.* **2013**, *24*, 593.
30. Rangari, V. K.; Hassan, T. A.; Zhou, Y.; Mahfuz, H.; Jeelani, S.; Prorok, B. C. *J. Appl. Polym. Sci.* **2007**, *103*, 308.
31. Auad, M. L.; Zhao, L.; Shen, H.; Nutt, S. R.; Sorathia, U. *J. Appl. Polym. Sci.* **2007**, *104*, 1399.
32. Lee, S. H.; Teramoto, Y.; Shiraishi, N. *J. Appl. Polym. Sci.* **2002**, *84*, 468.
33. Tseng, C. J.; Kuo, K. T. *J. Quant. Spectrosc. Radiat. Transfer* **2002**, *72*, 349.